Journal of Modern Optics, 2016
Vol. 63, No. 1, 46–49, http://dx.doi.org/10.1080/09500340.2015.1078919

A narrow-band speckle-free light source via random Raman lasing

Brett H. Hokr[a, b*], Morgan S. Schmidt[c], Joel N. Bixler [c, d], Phillip N. Dyer[b], Gary D. Noojin[b], Brandon Redding[e], Robert J. Thomas[c], Benjamin A. Rockwell[c], Hui Cao[e], Vladislav V. Yakovlev[a, d] and Marlan O. Scully[a, f, g]

[a]*Department of Phyics and Astronomy, Texas A&M University, College Station, TX, USA;* [b]*TASC Inc., San Antonio, TX, USA;* [c]*Optical Radiation Bioeffects Branch, Bioeffects Division, Human Effectiveness Directorate, 711th Human Performance Wing, JBSA Fort Sam, Houston, TX, USA;* [d]*Department of Biomedical Engineering, Texas A&M University, College Station, TX, USA;* [e]*Department of Applied Physics, Yale University, New Haven, CT, USA;* [f]*Department of Mechanical and Aerospace Engineering, Princeton University, Princeton, NJ, USA;* [g]*Department of Physics, Baylor University, Waco, TX, USA*

(*Received 28 February 2015; accepted 27 July 2015*)

Currently, no light source exists which is both narrowband and speckle free with sufficient brightness for full-field imaging applications. Light-emitting diodes are excellent spatially incoherent sources, but are tens of nanometers broad. Lasers, on the other hand, can produce very narrow-band light, but suffer from high spatial coherence which leads to speckle patterns, which distort the image. Here, we propose the use of random Raman laser emission as a new kind of light source capable of providing short-pulsed narrow-band speckle-free illumination for imaging applications.

Keywords: random Raman lasing; full-field imaging; speckle free; Raman scattering; turbid medium; ultra-fast strobe photography

1. Introduction

One of the biggest limitations of optical microscopy techniques for biological applications is speed. Laser-based microscopy techniques including Raman [1–10] and fluorescence [11–14] are limited to scanning pixel by pixel due to the speckle pattern of the laser caused by the large spatial coherence. To acquire high-resolution, megapixel-scale images at video rate (30 frames per second), one needs to have a pixel acquisition time of less than 33 ns. While laser sources with repetition rates in excess of this are readily available, often times, the signal level, detection equipment, and scanning rates of the laser cannot achieve sufficient speeds. Thus, to obtain real-time, dynamic information about the sample using a laser-based microscopy technique, one must sacrifice resolution, signal-to-noise, field of view, or all of the above.

Traditionally, the way around the issue of speckle is to use an incoherent light source such as an arc lamp [15] or light-emitting diodes [16] to do full-frame microscopy. However, such sources lack sufficient spectral radiance for Raman spectroscopy, and lack the temporal peak power to be used for any nonlinear optical effects. More recently, random lasing emission and highly multi-mode chaotic cavity lasers have been shown to provide light that is both bright and speckle free [17], but they are still broadband (typically tens of nanometers). That is, there is no existing light source capable of producing narrow-band, nanosecond-duration, speckle-free light. Random lasing via a narrow-band Raman transition, known as random Raman lasing (RRL) [18–21], provides a bright emission which is narrowband and has low spatial coherence.

Random lasing can be simply thought of as a laser in which feedback is provided by elastic scattering from a powder instead of the mirrors of a Fabry-Pérot [22]. Similar to traditional lasers, random lasers also have modes; however, random lasing modes are not as simple as transverse and longitudinal modes, and are usually more coupled than they would in a typical laser cavity [23]. This leads to strong mode competition and highly multi-mode emission. Each of these modes would produce its own independent speckle pattern, similar to passing a single-mode laser through a diffuser or multi-mode fiber, but because there are many independent modes, there are many speckle patterns superimposed which average out to provide a speckle-free emission very well suited for imaging [17,24]. This highly multi-mode nature that gives rise to the speckle-free emission also results in most of spontaneous emission bandwidth of the gain medium being used, making random lasers quite broadband. The use of barium sulfate ($BaSO_4$) as the Raman gain medium provides a narrow Raman linewidth of 8 cm^{-1}

*Corresponding author. Email: brett.hokr@tamu.edu

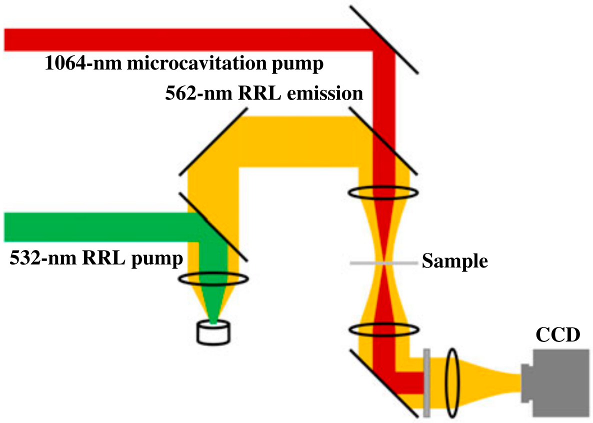

Figure 1. Schematic diagram of the experimental setup. (The color version of this figure is included in the online version of the journal.)

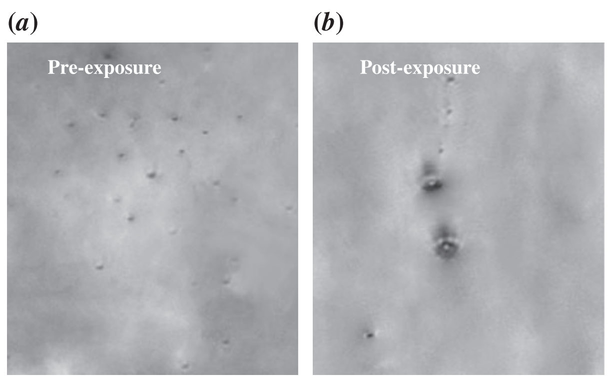

Figure 2. (*a*) Isolated bovine melanosomes before irradiation with the 1064-nm pulse. (*b*) Background subtracted melanosomes 125 ns after irradiation, displaying the formation of microcavitation bubbles. Both of these images were illuminated using RRL emission.

(0.25 nm at 562 nm), making the RRL emission both narrowband and speckle free [18,19]. In addition, RRL can be achieved at a wide range of wavelengths simply by changing the wavelength of the pump laser.

In this paper, we show that the light emitted from RRL is an entirely new kind of light source capable of producing very bright, narrow-band, temporally fast, and most importantly, speckle-free light. Such a source opens the possibility of a low spatial coherence light source while simultaneously allowing a relatively long temporal coherence due to the narrow bandwidth. Additionally, we will demonstrate stroboscopic images of microcavitation of melanosomes.

2. Results and discussion

In order to verify that RRL is indeed speckle free and may be used for strobe microscopy, the formation of bovine melanosome microcavitation bubbles was imaged. Melanin-containing organelles known as melanosomes are the main absorbing particles found in the monolayer of cells of the retinal pigment epithelium (RPE) layer of the retina [25,26]. The formation of small bubbles (microcavitation) is the primary retinal damage mechanism for laser pulses in the 10^{-9}–10^{-6} seconds range around the melanosomes in the RPE cells [27,28]. The formation of cavitation bubbles is highly correlated to cell death, and it is critical to understand the relationship between laser irradiance and damage. Using strobe microscopy, one can determine damage thresholds by imaging the cavitation events. Probit analysis, the standard technique for ascribing threshold values, was used to estimate the laser-induced damage (ED50) required to cause damage through microcavitation images [29,30]. Additional experimental details pertaining to the traditional use of strobe photography in microcavitation studies are discussed in Schmidt et al. [31].

For this experiment, shown schematically in Figure 1, two laser systems were needed in order to observe the microcavitation events after exposure. First, the RRL, made of $BaSO_4$ powder with particle diameters of 1–5 µm, was pumped with a frequency-doubled Spectra Physics Model GCR-130 Nd:YAG for an output of 532 nm at 10 Hz. From Mie scattering calculations, we can estimate the transport mean free path to be in the order of a few microns for the particle sizes that make up our sample, which is 1 cm in thickness, thousands of optical depths thick. The 532 nm beam was gently focused on the $BaSO_4$, with an approximate spot size of 1 mm. This optical spot size was determined through a previous study [18]. A lens was used to collimate the 562 nm emission from the $BaSO_4$ at a 45° angle. The beam was then directed toward the melanosome sample through a set of mirrors and through the back of an infrared mirror that turned the irradiation beam to the sample. Second, the illumination beam was co-aligned with the irradiation beam, which consisted of a 10 ns pulse duration from a 1064 nm Nd:YAG (spectra physics, INDI-30). Time-resolved imagery was achieved using a delay generator to control the delay between the irradiation beam and the illumination beam, as well as trigger the Bobcat CCD camera (Imperx Incorporated, Boca Raton, Florida) to capture an image. A long working distance microscope, 10× objective, was used with a 400-mm tube lens for a total magnification of 20× [31], providing micrometer spatial resolution and a nanosecond strobe with steps of nanoseconds relative to the laser illumination. Furthermore, the experimental setup allowed for the observation of microcavitation formation, as well as pre- and post-cavitation images. Background subtraction from the exposure image allowed for improved photographs of the cavitation events. The results are shown in Figure 2.

To more fully explore the spatial coherence properties of RRL emission, we have preformed a Young's double-slit experiment illuminated with three different light sources, RRL emission, elastically scattered 532 nm radiation from the pump laser, and a Helium–Neon laser for reference. In this experiment, the RRL was pumped with a 50-ps pulse

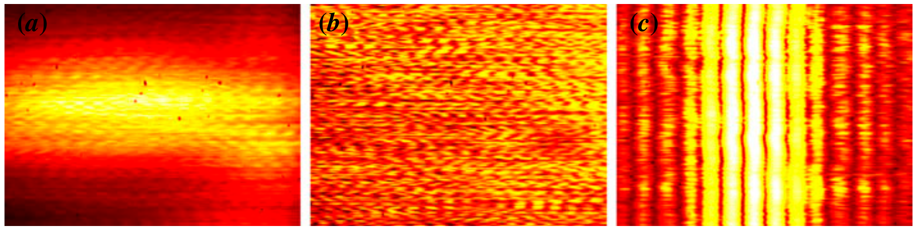

Figure 3. Double-slit diffraction pattern generated by (*a*) random Raman laser emission, (*b*) elastically scattered 532 nm pump, and (*c*) Helium–Neon laser. (The color version of this figure is included in the online version of the journal.)

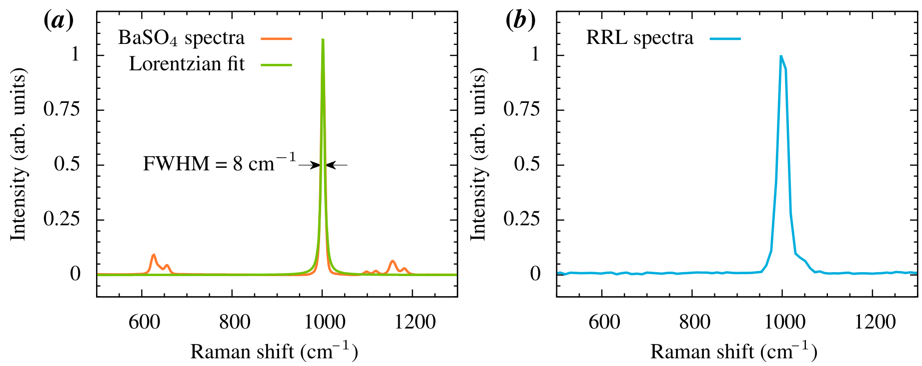

Figure 4. (*a*) Linewidth of the spontaneous Raman spectrum for $BaSO_4$. The Lorentzian fit gives the full width at half maximum width to be $8\,cm^{-1}$ (0.25 nm at 562 nm). (*b*) Spectrum of RRL emission. Note that this data-set was taken with a lower resolution spectrometer, such that the width of this peak is determined by the resolution of that spectrometer and not by the emission. (The color version of this figure is included in the online version of the journal.)

from a Spectra Physics Quanta-Ray GCR-3RA. The pulses had a pulse energy of 530 μJ and were gently focused to a beam diameter of 0.83 mm on the surface of the powder corresponding to an intensity approximately three times larger than the threshold required for RRL. The surface of the $BaSO_4$ powder was imaged to the double slit with 10× magnification in a 4-f arrangement. The two slits were 100 μm wide and separated by 350 μm. Following the slit, a cylindrical lens was used to image the vertical direction onto the CCD with unit magnification. Thus, this setup effectively probes the spatial coherence of two 10 μm thick lines on the surface of the powder separated by 35 μm. For the elastically scattered pump, the laser was attenuated well below the lasing threshold to avoid artifacts stemming from pump depletion. The Helium–Neon laser was obtained with the same lens arrangement to allow direct comparison.

The results of the double-slit experiment are shown in Figure 3. They clearly show that while a small amount of spatial coherence persists in the RRL emission, it is much less pronounced than even that of the elastically scattered pump radiation. This result can be understood most easily by thinking about it in terms of speckle patterns. If a single spatial mode laser is passed through a diffuser, it will generate a speckle pattern, but if this diffuser is rotated, these speckle patterns will average out over time to provide a uniform illumination. Each one of these speckle patterns can be thought of as a single mode of the laser diffuser system. In a highly multi-mode random laser, including the random Raman laser, each spatial mode of the laser generates a different speckle pattern for a given diffuser (elastic scattering in a random laser). These many speckle patterns average over all to provide a low coherence source. It should be noted that the spatial coherence properties of the random Raman laser emission showed no noticeable dependence on the pump laser power, suggesting that the random Raman laser is operating in a regime where the number of lasing modes is roughly saturated.

In addition to strobe photography applications, RRL emission could have applications as a spatially incoherent source for spectroscopy. Figure 4 shows that the spontaneous Raman spectrum for $BaSO_4$ has a spontaneous emission bandwidth of $8\,cm^{-1}$ for the strongest Raman line. This linewidth convoluted with the pump laser spectrum (in this case, it is sufficiently narrow that it can be neglected) provides the maximum possible bandwidth of the RRL much like the spontaneous emission bandwidth which would determine the maximum gain bandwidth of a laser. Additionally, the RRL emission spectrum is shown to illustrate the lack of the weaker Raman peaks seen in the spontaneous spectrum. The wider width of the RRL emission spectrum here is due to the fact that a lower resolution spectrometer was used to acquire this data. Thus, the width of this feature is determined solely by the resolution of the spectrometer and not by the RRL emission. The narrow

RRL linewidth would be sufficient for full-field Raman spectroscopy. Given the speckle-free nature combined with the narrow linewidth of the RRL emission, it would, in principle, be possible to acquire an entire Raman spectral image in a single laser shot. Even if many shots are required to obtain the required signal-to-noise, this would likely still far exceed the speed at which current imaging Raman microscopes can obtain spectroscopic images. The obvious limitation for such a technique is the lack of a spectrometer capable of detecting a Raman spectrum from each point in a two-dimensional array. Currently, no such detector exists; however, recent advances in compressive sensing offer hope in this area [32].

3. Conclusion

We have shown that random Raman laser emission is a unique source of light. It can be made very bright (a few percent of the pump energy), it is sufficiently narrowband for spectroscopic applications with a linewidth of at most $8\,cm^{-1}$, and, most importantly, it is sufficiently spatially incoherent, such that speckle-free full-frame images can be obtained. Additionally, we have acquired proof of principle images demonstrating speckle-free strobe photography images of microcavitation in bovine melanasomes using random Raman laser emission as the stroboscopic illumination source.

Acknowledgements

BHH would like to acknowledge a graduate fellowship from the Department of Defense Science, Mathematics and Research for Transformation (SMART) fellowship program. JNB and RJT would like to acknowledge support from AFRL 711 HPW.

Disclosure statement

No potential conflict of interest was reported by the authors.

Funding

This work was partially supported by National Science Foundation [grant number ECCS-1250360], [grant number DBI-1250361], [grant number CBET-1250363], [grant number PHY-1241032] (INSPIRE CREATIV), [grant number PHY-1068554], [grant number EEC-0540832] (MIRTHE ERC), and [grant number DMR-1205307]; the Robert A. Welch Foundation [Award A-1261]; and Research performed by TASC Inc. was conducted under USAF [contract number FA8650-14-D-6519].

ORCID

Joel N. Bixler http://orcid.org/0000-0002-9970-4141

References

[1] Freudiger, C.W.; Min, W.; Saar, B.G.; Lu, S.; Holtom, G.R.; He, C.; Tsai, J.C.; Kang, J.X.; Xie, X.S. *Science* **2008,** *322,* 1857–1861.

[2] Yakovlev, V.V.; Zhang, H.F.; Noojin, G.D.; Denton, M.L.; Thomas, R.J.; Scully, M.O. *Proc. Nat. Acad. Sci. USA* **2010,** *107,* 20335–20339.

[3] Beier, H.T.; Noojin, G.D.; Rockwell, B.A. *Opt. Express* **2011,** *19,* 18885–18892.

[4] Ozeki, Y.; Umemura, W.; Otsuka, Y.; Satoh, S.; Hashimoto, H.; Sumimura, K.; Nishizawa, N.; Fukui, K.; Itoh, K. *Nat. Photonics* **2012,** *6,* 845–851.

[5] Meng, Z.; Petrov, G.I.; Yakovlev, V.V. *Appl. Phys. B Lasers Opt.* **2013,** *112,* 99–103.

[6] Scully, M.O.; Kattawar, G.W.; Lucht, R.P.; Opatrnŷ, T.; Pilloff, H.; Rebane, A.; Sokolov, A.V.; Zubairy, M.S. *Proc. Nat. Acad. Sci. USA* **2002,** *99,* 10994–11001.

[7] Evans, C.L.; Potma, E.O.; Puoris'haag, M.; Côté, D.; Lin, C.P.; Xie, X.S. *Proc. Nat. Acad. Sci. USA* **2005,** *102,* 16807–16812.

[8] Petrov, G.I.; Arora, R.; Yakovlev, V.V.; Wang, X.; Sokolov, A.V.; Scully, M.O. *Proc. Nat. Acad. Sci. USA* **2007,** *104,* 7776–7779.

[9] Arora, R.; Petrov, G.I.; Yakovlev, V.V.; Scully, M.O. *Proc. Nat. Acad. Sci. USA* **2012,** *109,* 1151–1153.

[10] Camp, C.H., Jr.; Lee, Y.J.; Heddleston, J.M.; Hartshorn, C.M.; Walker, A.R.H.; Rich, J.N.; Lathia, J.D.; Cicerone, M.T. *Nat. Photonics* **2014,** *8,* 627–634.

[11] Denk, W.; Strickler, J.H.; Webb, W.W. *Science* **1990,** *248,* 73–76.

[12] Hell, S.W.; Wichmann, J. *Opt. Lett.* **1994,** *19,* 780.

[13] Helmchen, F.; Denk, W. *Nat. Methods* **2005,** *2,* 932–940.

[14] Horton, N.G.; Wang, K.; Kobat, D.; Clark, C.G.; Wise, F.W.; Schaffer, C.B.; Xu, C. *Nat. Photonics* **2013,** *7,* 205–209.

[15] Lichtman, J.W.; Conchello, J.A. *Nat. Methods* **2005,** *2,* 910–919.

[16] Albeanu, D.F.; Soucy, E.; Sato, T.F.; Meister, M.; Murthy, V.N. *PLoS One* **2008,** *3,* e2146.

[17] Redding, B.; Choma, M.A.; Cao, H. *Nat. Photonics* **2012,** *6,* 355–359.

[18] Hokr, B.H.; Bixler, J.N.; Cone, M.; Mason, J.D.; Beier, H.T.; Noojin, G.D.; Petrov, G.I.; Golovan, L.A.; Thomas, R.J.; Rockwell, B.A.; Yakovlev, V.V. *Nat. Commun.* **2014,** *5,* 4356.

[19] Hokr, B.H.; Bixler, J.N.; Noojin, G.D.; Thomas, R.J.; Rockwell, B.A.; Yakovlev, V.V.; Scully, M.O. *Proc. Nat. Acad. Sci.* **2014,** *111,* 12320–12324.

[20] Hokr, B.H.; Bixler, J.N.; Yakovlev, V.V. *Appl. Phys. A* **2014,** *117,* 681–685.

[21] Hokr, B.H.; Yakovlev, V.V.; Scully, M.O. *ACS Photonics* **2014,** *1,* 1322–1329.

[22] Cao, H.; Zhao, Y.G.; Ho, S.T.; Seelig, E.W.; Wang, Q.H.; Chang, R.P.H. *Phys. Rev. Lett.* **1999,** *82,* 2278–2281.

[23] Türeci, H.E.; Ge, L.; Rotter, S.; Stone, A.D. *Science* **2008,** *320,* 643–646.

[24] Mermillod-Blondin, A.; Mentzel, H.; Rosenfeld, A. *Opt. Lett.* **2013,** *38,* 4112–4115.

[25] Lin, C.P.; Kelly, M.W. *Appl. Phys. Lett.* **1998,** *72,* 2800.

[26] Lee, H.; Alt, C.; Pitsillides, C.M.; Lin, C.P. *J. Biomed. Opt.* **2007,** *12,* 064034.

[27] Lund, B.J.; Lund, D.J.; Edsall, P.R.; Gaines, V.P. *J. Biomed. Opt.* **2014,** *19,* 105006.

[28] Brinkmann, R.; Hüttmann, G.; Rögener, J.; Roider, J.; Birngruber, R.; Lin, C.P. *Lasers Surg. Med.* **2000,** *27,* 451–464.

[29] Cain, C.P.; Noojin, G.D.; Manning, L. USAF Armstrong Lab. 1996, *AL/OE-TR-1996-0102*.

[30] Finney, D.J. *Probit Analysis*. *3*, Cambridge University Press: New York, 1971.

[31] Schmidt, M.S.; Kennedy, P.K.; Vincelette, R.L.; Denton, M.L.; Noojin, G.D.; Schuster, K.J.; Thomas, R.J.; Rockwell, B.A. *J. Biomed. Opt.* **2014,** *19,* 35003.

[32] Gao, L.; Liang, J.; Li, C.; Wang, L.V. *Nature* **2014,** *516,* 74–77.